lawn of 2 hours. Average light intensity at canopy (1 m from lights) was 294 $\mu m\ s^{-1}\ m^{-2}$. Pot volume was 0.4 $m^3$; the initial soil, 0.1 $m^3$ of gravel, was topped with 0.3 $m^3$ of 40:60 sand–Surrey loam mix (41.61 ppm nitrogen, 17.63 ppm phosphorus, 12.45 ppm potassium). Temperature varied smoothly between a maximum of 20°C during the day and a minimum of 12°C at night. Relative humidity varied smoothly between a maximum of 70% after watering and a minimum of 58%.

19. Following the "moderate" Intergovernmental Panel for Climate Change scenario for 2060 [J. T. Houghton *et al.*, Eds., *Climate Change 1995. The Science of Climate Change* (Cambridge Univ. Press, Cambridge, 1996)].
20. The experimental chambers were in two banks of eight (all statistical analyses have $n = 8$ for each treatment). The design of the Ecotron is such that the eight chambers in one bank are not statistically independent replicates. However, because each chamber receives air from only the air-handling unit associated with that bank and is physically sealed and separated from adjacent chambers in the bank, the chambers are effectively independent. So that we could be certain that $CO_2$ effects were not confounded by unexpected bank effects, the main experiment (run 1, 9 months, three plant generations) was repeated for 4.5 months (run 2, 1.5 plant generations) with the position of the experimental treatments interchanged between consecutive runs. No bank effects were detected. In addition, in later experiments (*21*) we also repeated both the ambient (run 3) and the elevated (run 4) $CO_2$ in one bank while manipulating temperature in the other bank, always for 9 months. In all runs, results obtained with a particular $CO_2$ treatment were similar. For simplicity, we concentrate here on the results from run 1 with corroborating information only from later runs. An artificial "winter" was imposed by cutting most of the above-ground vegetation at the end of each generation and replacing it immediately as litter.
21. L. J. Thompson, K. Sanbrooke, S. E. Hartley, unpublished data; T. M. Bezemer, T. H. Jones, K. J. Knight, unpublished data; S. E. Hartley *et al.*, unpublished data.
22. Infrared gas analyzer measurements were taken as flux (in ppm $CO_2$) over 48-hour periods with an airflow of 0.25 $m^3$ per second per chamber.
23. Three of the plant species (*Cardamine hirsuta*, *Senecio vulgaris*, and *Spergula arvensis*) showed increased rates of photosynthesis during the course of the experiment; there was no significant change in the rate of photosynthesis of *Poa annua*. Elevated $CO_2$ also resulted in significant differences in the plant populations that were both species and generation dependent. Herbivores showed species-specific changes: For example, in run 1, *Brevicoryne brassicae* populations at the end of the second plant generation were higher in ambient $CO_2$ than in elevated $CO_2$. The reverse was true for *Myzus persicae* at the end of the third plant generation.
24. C. Körner and J. A. Arnone III, *Science* **257**, 1672 (1992).
25. J. N. Klironomos and B. Kendrick, *Plant Soil* **170**, 183 (1995).
26. C. Kampichler *et al.*, *Global Change Biol.* **4**, 335 (1998).
27. Root carbon and nitrogen contents were determined in a Carlo Erba NA 1500 elemental analyzer. Mean (± SE) C:N ratios in run 1 were as follows: 0 to 10 cm, 34.5 (±1.1):1 (ambient), 36.1 (±1.2):1 (elevated), $P = 0.351$; 10 to 20 cm, 41.9 (±3.5):1 (ambient), 35.0 (±1.0):1 (elevated), $P = 0.068$.
28. C. W. Rice *et al.*, *Plant Soil* **165**, 67 (1994).
29. J. N. Klironomos, M. C. Rilling, M. F. Allen, *Funct. Ecol.* **10**, 527 (1996).
30. Enzyme activities measured were urease, xylanase, trehalase, and arginine deaminase [F. Schinner *et al.*, *Methods in Soil Biology* (Springer, Heidelberg, 1996)]. See (*18*) for details.
31. Soil was initially sterilized by methyl bromylation. Each replicate then received 120 ml of a microbial inoculum prepared from 20- to 25-μm pore filtrate (Whatman number 4) of Silwood Park soil. This treatment also introduced nematodes and protists to all chambers [see (*16, 17*)].
32. R. I. Amann, W. Ludwig, K. H. Schleifer, *Microbiol. Rev.* **59**, 143 (1995). DNA was extracted directly from 1 g of each soil sample [K. D. Bruce *et al.*, *Mol. Ecol.* **4**, 605 (1995)]. The polymerase chain reaction (PCR) was used to amplify eubacteria 16S ribosomal RNA genes present in the extracted DNA with fluorescently labeled universal eubacterial oligonucleotide primers pA and pH′ [U. Edwards *et al.*, *Nucleic Acids Res.* **17**, 7843 (1989)]. PCR products were digested with the restriction endonuclease Hae III, separated with an ABI 373 A automated DNA sequencer, and analyzed with Genotyper software (version 1.1). The resulting profiles, each peak of which identifies a different variant, were compared visually.
33. Soil samples from all chambers were inoculated onto agar plates, using 10 different protocols. Colony numbers and identities were ascertained after varying periods of incubation. Only the cellulose agar (for cellulolytic fungi) showed statistically significant differences [mean (± SE) number of colonies ($\times 10^2$ $g^{-1}$ soil) recovered, 17.2 (±9.4) (ambient), 35.0 (±14.8) (elevated); $P < 0.05$] between the ambient and elevated $CO_2$ treatments.
34. Measured as cotton rotting rate [M. O. Hill, P. M. Latter, G. Bancroft, *Can. J. Soil Sci.* **65**, 609 (1985)]. For run 1, this value was 36.5 cotton strips per year ± 3.53 (elevated) and 26.2 cotton strips per year ± 4.20 (ambient); $P < 0.05$.
35. We used a randomization test on the observed distribution of fungal species against distributions from a null model in which each of the 33 species was randomly assigned to one of the two treatments a total of $n$ times ($n$ = the number of chambers it occupied in the experiment). The probability that each occurrence of a species was assigned to each treatment was 0.5 and did not depend on the number of times the species had already been assigned to that treatment. A maximum of eight occurrences per species per treatment was allowed. The null model was run for a total of 5000 iterations. Not once did the null model yield as few as 14 species common to both treatments (the minimum was 23), or as many as 9 restricted to a single treatment (the maximum was 6) (two-tailed $P < 0.001$).
36. G. I. Ågren and E. Bosatta, *Ecology* **68**, 1181 (1987); G. I. Ågren *et al.*, in *Effects of Climate Change on Grasslands and Coniferous Forests*, J. M. Melillo and A. Breymeyer, Eds. (Wiley, Chichester, UK, 1996), pp. 207–228.
37. E. G. O'Neill, R. J. Luxmoore, R. J. Norby, *Can. J. For. Res.* **17**, 878 (1987); K. Ineichen, V. Wiemken, A. Wiemken, *Plant Cell Environ.* **18**, 703 (1995); G. M. Bernston and F. A. Bazzaz, *Plant Soil* **187**, 119 (1996); D. L. Godbold and G. M. Bernston, *Tree Physiol.* **17**, 347 (1997).
38. S. P. Hopkins, *Biology of the Springtails. Insecta: Collembola* (Oxford Univ. Press, Oxford, 1997). *Folsomia candida* is also reported to feed on nematodes [Q. Lee and P. Widden, *Soil Biol. Biochem.* **28**, 689 (1996); S. Visser and J. B. Whittaker, *Oikos* **29**, 320 (1977); D. Parkinson, S. Visser, J. B. Whittaker, *Soil Biol. Biochem.* **11**, 529 (1979); R. D. G. Hanlon, *Oikos* **36**, 362 (1981); R. D. Bardgett, J. B. Whittaker, J. C. Frankland, *Biol. Fertil. Soils* **16**, 296 (1993); (*25*)].
39. J. C. Moore and P. C. De Ruiter, in *Multitrophic Interactions in Terrestrial Systems*, A. C. Gange and V. K. Brown, Eds. (Blackwell Scientific, Oxford, 1977), pp. 375–393.
40. H. H. Rogers, S. A. Prior, E. G. O'Neill, *Crit. Rev. Plant Sci.* **11**, 251 (1992); H. A. Torbert, S. A. Prior, H. H. Rogers, *Soil Sci. Soc. Am. J.* **59**, 1321 (1995); A. S. Ball, *Global Change Biol.* **3**, 379 (1997); E. Paterson *et al.*, *ibid.*, p. 363; J. N. Klironomos *et al.*, *ibid.*, p. 473.
41. Experiments were partially funded by the NERC TIGER Initiative (GST/02/646), the British Council (VIE/891/11), and the Austrian Academy of Sciences (ICBP-11/95). Various colleagues, too numerous to list, have contributed to the experiment. In particular, we thank G. Couper, R. Greenwood, C. Jerram, K. Knight, J. Newington, K. Sanbrooke, P. Small, and D. Wildman for their support and enthusiasm. We thank F. Bazzaz, C. Godfray, and P. Groffman for commenting on earlier versions of the manuscript.

15 October 1997; accepted 29 January 1998

# Control of Alternative Splicing of Potassium Channels by Stress Hormones

Jiuyong Xie and David P. McCobb*

Many molecular mechanisms for neural adaptation to stress remain unknown. Expression of alternative splice variants of *Slo*, a gene encoding calcium- and voltage-activated potassium channels, was measured in rat adrenal chromaffin tissue from normal and hypophysectomized animals. Hypophysectomy triggered an abrupt decrease in the proportion of Slo transcripts containing a "STREX" exon. The decrease was prevented by adrenocorticotropic hormone injections. In *Xenopus* oocytes, STREX variants produced channels with functional properties associated with enhanced repetitive firing. Thus, the hormonal stress axis is likely to control the excitable properties of epinephrine-secreting cells by regulating alternative splicing of Slo messenger RNA.

Stressors including cold exposure, hypoglycemia, and physical constraint trigger adaptive changes in catecholamine- and peptide-secreting chromaffin cells of the adrenal medulla. Rapid stress-induced increases in transcription of the epinephrine-synthesizing enzyme phenylethanolamine-*N*-methyltransferase (PNMT) result from direct interaction of receptor-bound glucocorticoid stress hormones with glucocorticoid response elements in the promoter (*1*). Glucocorticoids also regulate transcription of voltage-gated K channel genes in cardiac and pituitary cells (*2*). In chromaffin cells, large-conductance "BK" calcium- and voltage-gated K channels are particularly prominent, participating in action po-

Section of Neurobiology and Behavior, Cornell University, Ithaca, NY 14853, USA.

*To whom correspondence should be addressed. E-mail: dpm9@cornell.edu

tential repolarization and driving the brief afterhyperpolarization. Pronounced differences in the repetitive firing properties of chromaffin cells have been attributed to variations in kinetics and voltage dependence of BK channel gating in these cells (*3*, *4*). *Slo* is the only known gene encoding BK channels, and alternative splicing may underlie much of the existing BK functional diversity (*5*, *6*).

Hypophysectomy (pituitary removal) in rats represents a robust and reproducible experimental nullification of hormonal stress axis function and has confirmed results with other approaches demonstrating extensive stress-related plasticity in chromaffin cell phenotype (*7*). We used a quantitative reverse transcription polymerase chain reaction (RT-PCR) strategy (*8*) to measure in parallel the effects of hypophysectomy (*9*) on adrenal medullary levels of PNMT and total rat Slo (rSlo) mRNA (without regard to splicing variation). PNMT mRNA was reduced to 8.5 ± 1.1% (±SEM; $N = 4$) of normal levels by hypophysectomy, whereas total Slo mRNA was not detectably altered over 10 weeks after hypophysectomy.

Five alternative splice sites have been identified in the COOH-terminal half of mammalian *Slo* genes (*5*, *10*, *11*). Using RT-PCR on adrenal medulla, we found no inserts at sites I, III, or IV (Fig. 1A). However, primers bracketing sites I to III yielded two distinct bands. Subcloning and sequencing indicated that the lower molecular weight band contained only products with no insert at site II (configuration referred to as ZERO). Two related variants of similar size composed the upper band, referred to as STREX-1 and -2 (stress axis–regulated exons). The STREX variants share a 174–base pair (bp) exon (*10*, *11*), with STREX-2 having an additional 9-bp exon (Fig. 1B).

The relative intensities of STREX and ZERO PCR product bands were very consistent between reactions from the same sample, providing an internal calibration system for measuring relative abundance across treatment groups (*12*). The ratio of STREX to ZERO forms was markedly reduced by hypophysectomy (Fig. 2). In six unoperated animals, the ratio varied from 0.59 to 0.83 (mean ± SEM = 0.74 ± 0.02) (Fig. 2B). In 14 rats hypophysectomized 15 days earlier, the ratio varied from 0.13 to 0.39 (mean = 0.25 ± 0.005). Thus, ranges did not overlap, and means differed very significantly ($P < 0.00002$). In a separate series of reactions, we measured a decrease in the abundance of STREX relative to total RNA using STREX-specific primers and a STREX-derived calibration template ($P < 0.0002$). No other variants between the obligatory primer sites were detected in adrenal medulla by us or others (*10*). Because total Slo transcript was not changed by hypophysectomy, the change described likely reflects a decrease in the absolute abundance of STREX with an accompanying increase in ZERO.

The STREX to ZERO ratio declined rapidly after hypophysectomy (Fig. 2E). By 11 days, it was 42.5% of normal ($P = 0.002$), and by 32 days, it was 11.5% of normal, indistinguishable from the value at 70 days. Thus, the time course of STREX

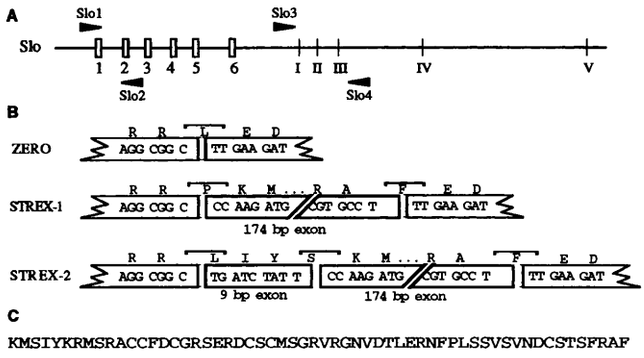


**Fig. 1.** Structure of mammalian Slo mRNAs. (**A**) Roman numerals indicate five alternative splice sites downstream of the six transmembrane domains common to voltage-gated $K^+$ channels (boxes). PCR primers Slo1 and Slo2 spanning a non–alternatively spliced junction were used to measure total Slo transcript amounts in adrenal medullary RNA. Slo3 and Slo4 revealed inserts at site II only. (**B**) Three variants at site II. ZERO had no insert between the flanking exons. Nucleotide sequence of STREX-1 dictates the substitution of P for L, followed by the insertion of 58 residues. The sequence of STREX-2 dictates the insertion, after L, of 61 residues, the downstream 58 of which are shared with STREX-1 at nucleotide and amino acid levels (**C**). Boxed segments demarcate midcodon splice boundaries providing the most parsimonious explanation for the observed sequences. In STREX-2, a 9-bp exon is presumably inserted before the 174-bp exon in STREX-1. Insertion of this 9-bp exon alone can account for a variant identified in other tissues (*6*) having residues IYF following L. Single-letter abbreviations for the amino acid residues are as follows: A, Ala; C, Cys; D, Asp; E, Glu; F, Phe; G, Gly; I, Ile; K, Lys; L, Leu; M, Met; N, Asn; P, Pro; R, Arg; S, Ser; T, Thr; V, Val; and Y, Tyr.

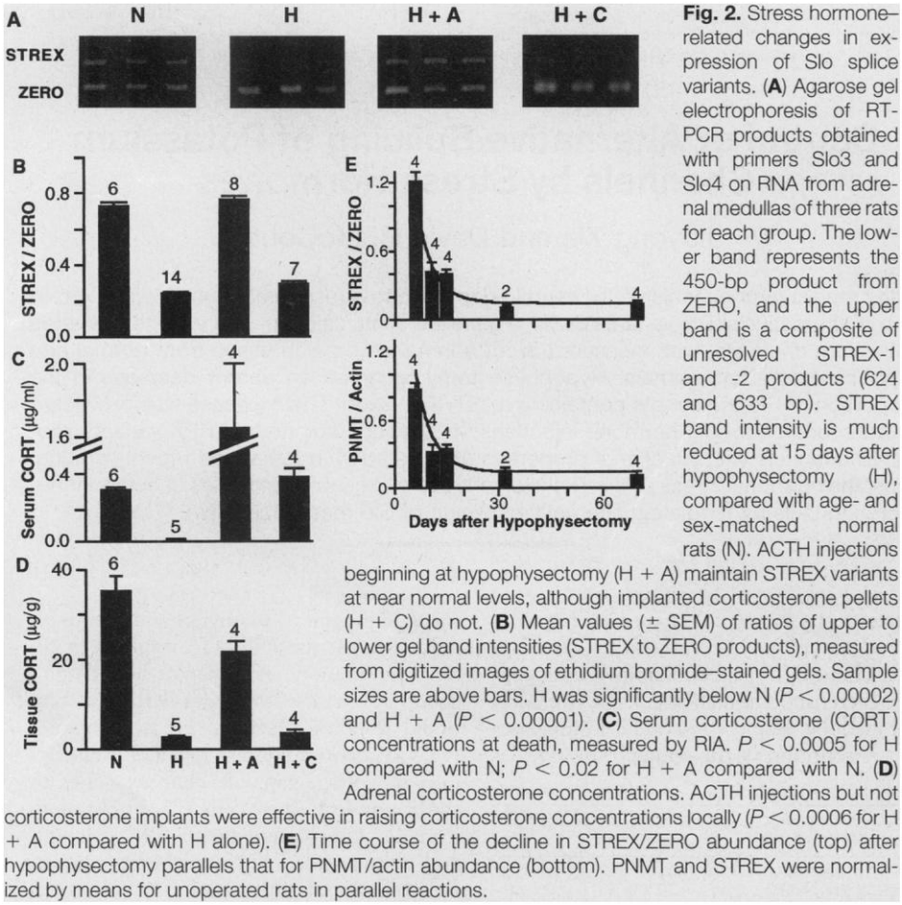


**Fig. 2.** Stress hormone–related changes in expression of Slo splice variants. (**A**) Agarose gel electrophoresis of RT-PCR products obtained with primers Slo3 and Slo4 on RNA from adrenal medullas of three rats for each group. The lower band represents the 450-bp product from ZERO, and the upper band is a composite of unresolved STREX-1 and -2 products (624 and 633 bp). STREX band intensity is much reduced at 15 days after hypophysectomy (H), compared with age- and sex-matched normal rats (N). ACTH injections beginning at hypophysectomy (H + A) maintain STREX variants at near normal levels, although implanted corticosterone pellets (H + C) do not. (**B**) Mean values (± SEM) of ratios of upper to lower gel band intensities (STREX to ZERO products), measured from digitized images of ethidium bromide–stained gels. Sample sizes are above bars. H was significantly below N ($P < 0.00002$) and H + A ($P < 0.00001$). (**C**) Serum corticosterone (CORT) concentrations at death, measured by RIA. $P < 0.0005$ for H compared with N; $P < 0.02$ for H + A compared with N. (**D**) Adrenal corticosterone concentrations. ACTH injections but not corticosterone implants were effective in raising corticosterone concentrations locally ($P < 0.0006$ for H + A compared with H alone). (**E**) Time course of the decline in STREX/ZERO abundance (top) after hypophysectomy parallels that for PNMT/actin abundance (bottom). PNMT and STREX were normalized by means for unoperated rats in parallel reactions.

decline was very similar to that for PNMT mRNA.

Pituitary influence on chromaffin cells is generally indirect, with adrenocorticotropic hormone (ACTH) acting on cortical cells to stimulate the synthesis of glucocorticoids, which then act on chromaffin cells. Subcutaneous injections of ACTH (4 U/100 g) (*13*) were given daily or on alternate days beginning at surgery to determine whether the effects of hypophysectomy could be prevented by ACTH replacement. Fifteen days after surgery, ratios of STREX to ZERO products were indistinguishable from normal animals and significantly higher than those of vehicle-injected or uninjected hypophysectomized animals (Fig. 2B).

Attempts to bypass ACTH by directly manipulating corticosteroid concentrations in the blood were ineffective in controlling STREX variant expression. Neither dexamethasone injections 81 days after surgery (10 mg $kg^{-1}$ $day^{-1}$ for 4 days) nor implantation of corticosterone pellets (the major rat adrenal glucocorticoid under ACTH control) at surgery raised or maintained STREX levels significantly above hypophysectomized levels. One explanation is that injections and implants, although restoring serum corticosterone concentrations, cannot match the much higher local concentrations to which chromaffin cells are exposed in cortico-medullary venous sinuses within the gland (*14*). To address this question, we used radioimmunoassay (RIA) (*15*) to measure serum corticosterone concentrations and total gland corticosterone content. Normal and hypophysectomized rat sera contained 312 ± 22 and 20 ± 6 ng/ml, respectively (Fig. 2D). Corticosterone was roughly 100-fold more concentrated in adrenal tissue than in serum (Fig. 2D). Corticosterone implants (100 mg of pellet implanted subcutaneously at surgery) raised serum concentrations to 121 ± 14% of normal but raised adrenal content to only 10 ± 2% of normal. By contrast, ACTH injections raised serum concentrations to 529 ± 113% and adrenal content to 61 ± 7% of normal. They also prevented the cortical atrophy normally caused by hypophysectomy. Thus, ACTH injections maintained high local concentrations (with supernormal secretory rates) apparently required to maintain near normal STREX levels after hypophysectomy.

We estimated the relative abundance of STREX and ZERO transcripts in native tissue by correcting for differences in PCR amplification efficiencies, assuming similar RT efficiencies. To measure amplification efficiencies, we constructed a plasmid containing both ZERO and STREX-2 isoforms, ensuring a one to one template ratio. Amplification yielded band intensity ratios (STREX to ZERO) of 0.64 ± 0.2 (STREX efficiency = 97% of ZERO efficiency per cycle). The ratio was negligibly affected by template amount, even when 100-fold greater than in tissue samples, indicating amplification within the linear range. Extrapolating from relative efficiencies, the STREX to ZERO template ratio in normal rats was 1.16. For hypophysectomized and ACTH-injected hypophysectomized rats, this ratio was 0.47 and 1.17, respectively, at 15 days. With the assumption that no other variants at site II occur in significant proportions in chromaffin cells, STREX variants made up about 53, 32, and 54% of total Slo transcripts in the respective groups. By 70 days, STREX transcripts declined to 15% of the total.

To determine whether STREX exons affect the functional properties of Slo channels, we constructed Slo expression plasmids differing only at site II, having the form of STREX-1, STREX-2, or ZERO (no inserts at sites I, III, and IV) (*16*). Currents in inside-out patches pulled from STREX cRNA-injected *Xenopus* oocytes (*17*) activated at voltages ~20 mV negative to those in ZERO-injected oocytes (Fig. 3) (*10*, *18*). At 10 μM intracellular $Ca^{2+}$ concentration ($[Ca^{2+}]_i$), the half-activation voltage ($V_{0.5}$, from Boltzmann fits) was −2.33 ± 0.30 mV for 25 STREX patches and 20.5 ± 1.44 mV for 8 ZERO patches. The steepness of voltage dependence did not differ (17.1 ± 0.5 mV/*e*-fold change for STREX, 16.2 ± 1.2 for ZERO). In addition, STREX speeds activation and slows deactivation at a given test potential. Slower BK deactivation has been linked to enhanced repetitive firing in chromaffin cells. Time constants of tail current kinetics (+90 to −80 mV) averaged 2.31 ± 0.06 and 0.85 ± 0.06 ms for 18 STREX and 7 ZERO patches, respectively.

Studies of firing properties and BK channels in native rat chromaffin cells (*3*, *4*) suggest that STREX exons enhance repetitive firing. Chromaffin cells subdivide into two types, those spiking continuously with a sustained current injection and those spiking only once or twice. BK channels in the former exhibit substantially slower deactivation kinetics. This slower kinetics enhances repetitive firing by augmenting the afterhyperpolarization, facilitating recovery from inactivation of sodium and calcium channels. Both more negative and faster activation will further augment the afterhyperpolarization by increasing BK openings during the brief action potential. It has been proposed that chromaffin cells secreting epinephrine rather than norepinephrine fire repetitively (*3*). Because the pattern of glucocorticoid receptor expression maps onto that for PNMT expression (*19*), we hypothesize that STREX is differentially expressed in epinephrine- and norepinephrine-secreting cells.

Our observation that stress hormones affect Slo mRNA composition suggests that hypophysectomy and more natural stress system perturbations will alter chromaffin BK channel protein composition and cellular excitability. For PNMT, protein levels and enzyme activity are not always commensurate with mRNA fluctuations, as translational and later stages are subject to additional regulatory controls (*20*). Howev-

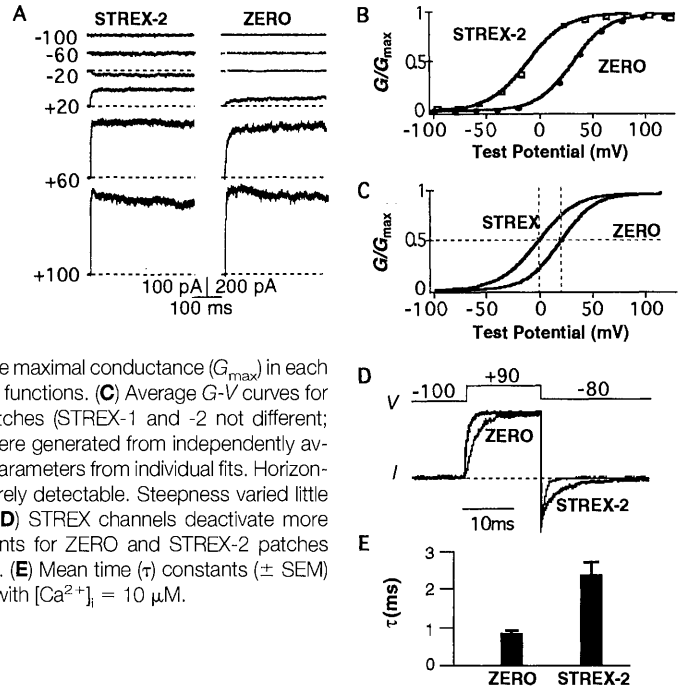


**Fig. 3.** Functional differences in Slo splice variants. (**A**) STREX-2 channels activate at more negative voltages than ZERO channels. Representative currents activated from a holding potential of −100 mV in inside-out patches from cRNA-injected *Xenopus* oocytes. $[Ca^{2+}]_i$ = 100 μM. (**B**) Conductance-voltage (*G-V*) relations for patches in (A). *G* values were normalized by the maximal conductance ($G_{max}$) in each patch and fit with Boltzmann functions. (**C**) Average *G-V* curves for 25 STREX and 8 ZERO patches (STREX-1 and -2 not different; $[Ca^{2+}]_i$ = 10 μM). Curves were generated from independently averaged $V_{0.5}$ and steepness parameters from individual fits. Horizontal SEM bars for $V_{0.5}$ are barely detectable. Steepness varied little within or between groups. (**D**) STREX channels deactivate more slowly, as seen in tail currents for ZERO and STREX-2 patches $[Ca^{2+}]_i$ = 100 μM. *I*, current. (**E**) Mean time (τ) constants (± SEM) from exponential fits to tails with $[Ca^{2+}]_i$ = 10 μM.

er, even small changes in STREX expression producing subtle changes in chromaffin cell excitability could have pronounced effects on the secretion of catecholamines and other products (including corticosteroids through reciprocal interactions with the adrenal cortex) (*21*), with potentially far-reaching consequences in humans. Among the functions likely to be affected to some extent are cardiovascular, digestive, metabolic, immune, and mental functions (*22*). Changes in chromaffin BK channels in response to hormonally communicated stress represent another dimension of stress-related plasticity in adrenal tissue.

Tissue-specific and developmental regulation of alternative splicing is well established for many genes, with factors and mechanisms being worked out. Reports of dynamic regulation of splicing patterns in adult tissues are rare (*23*). Exons in complex modular proteins such as ion channels often comprise discrete functional units, and dynamic hormonal control of exon selection provides a unique dimension for regulating the often critical functional nuances of the whole protein.

## REFERENCES AND NOTES


1. M. E. Ross *et al.*, *J. Neurosci.* **10**, 520 (1990); S. N. Ebert *et al.*, *J. Biol. Chem.* **269**, 20885 (1994).
2. E. S. Levitan, K. M. Hershman, T. G. Sherman, K. Takimoto, *Neuropharmacology* **35**, 1001 (1996); K. Takimoto and E. S. Levitan, *Circ. Res.* **75**, 1 (1994); K. Takimoto, A. F. Fomina, R. Gealy, J. S. Trimmer, E. S. Levitan, *Neuron* **11**, 359 (1993); B. Attardi, K. Takimoto, R. Gealy, C. Severns, E. S. Levitan, *Receptors Channels* **1**, 287 (1993).
3. C. R. Solaro, M. Prakriya, J. P. Ding, C. J. Lingle, *J. Neurosci.* **15**, 6110 (1995).
4. C. J. Lingle, C. R. Solaro, M. Prakriya, J. P. Ding, *Ion Channels* **4**, 261 (1996).
5. A. Butler, S. Tsunoda, D. P. McCobb, A. Wei, L. Salkoff, *Science* **261**, 221 (1993); J. Tseng-Crank *et al.*, *Neuron* **13**, 1315 (1994).
6. J. P. Adelman *et al.*, *Neuron* **9**, 209 (1992); N. S. Atkinson, G. A. Robertson, B. Ganetzky, *Science* **253**, 551 (1991).
7. M. K. Stachowiak, R. J. Rigual, P. H. K. Lee, O. H. Viveros, J. S. Hong, *Mol. Brain Res.* **3**, 275 (1988); E. Viskupic *et al.*, *J. Neurochem.* **63**, 808 (1994).
8. J. Xie, P. Lappas, W. Yao, E. Carpenter-Hyland, D. P. McCobb, *Soc. Neurosci. Abstr.* **22**, 402 (1996). For calibrated RT-PCR, different amounts of calibrator template cRNA {constructed as per S. Diviacco *et al.* [*Gene* **122**, 313 (1992)]} were added to identical 12.5-ng samples of tissue RNA. Relative PCR product band intensity was measured with BIT Image 1.55 (Digital Imagers, Elburn, IL). We measured the native template by extrapolating to the calibrator template amount yielding equivalent product bands, with corrections for length effects on amplification efficiency and band intensity.
9. Sprague-Dawley rats (Charles River) were hypophysectomized with the parapharyngeal approach to the occipitosphenoid suture. After trephination, the hypophysis was removed by aspiration. Hypophysectomized rats received 5% sucrose water. Marked reductions in adrenal cortical volume and rat body weight at death, compared with age- and sex-matched rats, indicated successful hypophysectomy.
10. M. Saito, C. Nelson, L. Salkoff, C. J. Lingle, *J. Biol. Chem.* **272**, 11710 (1997).
11. J. Ferrer, J. Wasson, L. Salkoff, M. A. Permutt, *Diabetologia* **39**, 891 (1996).
12. J. Xie and D. P. McCobb, *Soc. Neurosci. Abstr.* **23**, 309 (1997). The ratio of STREX to ZERO isoform varied only slightly more between left and right glands from a single animal ($N$ = 14 pairs) than between replicate measures on a single mRNA sample, supporting the quantitative reproducibility of the approach. Total RNA was extracted from dissected adrenal medullas, and 200 ng was used in a 10-μl RT reaction with 200 U of Superscriptase II and oligo$(dT)_{22}$ (Gibco BRL). One microliter of RT product was used in a 25-μl PCR for 30 cycles at 94°C, 30-s denaturation; 55°C, 30-s annealing; and 72°C, 30-s extension. Five microliters of product was run on a 2% agarose gel stained with ethidium bromide.
13. ACTH was in gel form (Rhone Poulenc Rorer Pharmaceutical, Collegeville, PA).
14. R. E. Coupland, *The Natural History of the Chromaffin Cell* (Longmans, London, 1965); R. J. Wurtman and J. Axelrod, *J. Biol. Chem.* **241**, 2301 (1966).
15. IMMUCHEM Double Antibody Corticosterone RIA kit (ICN, Irvine, CA) was used by the veterinary diagnostic lab at Cornell University. Corticosterone was extracted from ground adrenals with 0.5 ml of ethyl acetate at room temperature and spun at 11,000 rpm for 5 min, and the upper phase was saved, vacuum dried, and resuspended in 400 μl of resuspension buffer with 5% ethanol.
16. Plasmid constructs for cRNA expression in *Xenopus* oocytes were devised by modification of a mouse Slo (mSlo) expression construct (*5*). Rat adrenal RT-PCR products corresponding to ZERO, STREX-1, and STREX-2 variants were made with primers rSlo3 and a downstream primer with an internal Xho I site (sequence: 5′-ACCGCTCGAGCTCTGGCGTGGCTCCTCCTG-3′) and cloned into unique Hind III and Xho I sites in the mSlo vector. Restriction analysis and sequencing were used to confirm constructs. mSlo differs from rSlo outside the rat insert at only 4 of 716 residues. Plasmids were linearized with Sal I and transcribed with Ambion T3 mMESSAGE kit.
17. Patch clamp solutions were potassium methanesulfonate based (pH 7.0). Free calcium concentrations were determined with a calcium-selective electrode (Orion, Beverly, MA). Procedure and solutions were as described by D. P. McCobb *et al.* [*Am. J. Physiol.* **269**, H767 (1995)]. A List EPC-7 patch clamp with ITC-16 data interface (Instrutech, NY) and Pulse software (HEKA, Lambrecht, Germany) were used for data acquisition.
18. D. P. McCobb, J. Xie, D. Baro, *Soc. Neurosci. Abstr.* **23**, 1477 (1997).
19. S. Ceccatelli, A. Dagerlind, M. Schalling, A.-C. Wikstorm, *Acta Physiol. Scand.* **137**, 559 (1989).
20. D. L. Wong, A. Lesage, B. Siddall, J. W. Funder, *FASEB J.* **6**, 3310 (1992); D. L. Wong, R. J. Hayashi, R. D. Ciaranello, *Brain Res.* **330**, 209 (1985).
21. G. G. Nussdorfer, *Pharmacol. Rev.* **48**, 495 (1996).
22. R. C. Lake and M. G. Ziegler, *The Catecholamines in Psychiatric and Neurologic Disorders* (Butterworth, Stoneham, MA, 1985).
23. J. E. Kraus, J. V. Nadler, J. O. McNamara, *Mol. Brain Res.* **41**, 97 (1996).


24. We thank R. Harris-Warrick, D. Baro, R. Knapp, A. Bass, and R. Hoy for helpful discussions. Supported by the American Heart Association.

25 November 1997; accepted 23 February 1998


# Maternal Control of Embryogenesis by *MEDEA*, a *Polycomb* Group Gene in *Arabidopsis*


Ueli Grossniklaus,* Jean-Philippe Vielle-Calzada, Marilu A. Hoeppner, Wendy B. Gagliano†



The gametophytic maternal effect mutant *medea* (*mea*) shows aberrant growth regulation during embryogenesis in *Arabidopsis thaliana*. Embryos derived from *mea* eggs grow excessively and die during seed desiccation. Embryo lethality is independent of the paternal contribution and gene dosage. The *mea* phenotype is consistent with the parental conflict theory for the evolution of parent-of-origin–specific effects. *MEA* encodes a SET domain protein similar to *Enhancer of zeste*, a member of the *Polycomb* group. In animals, *Polycomb* group proteins ensure the stable inheritance of expression patterns through cell division and regulate the control of cell proliferation.


The plant life cycle alternates between diploid and haploid generations, sporophyte and gametophyte, as the haploid spores undergo several cell divisions before the gametes finally differentiate and fuse to produce the diploid zygote. We identified an *Arabidopsis thaliana* mutant, *medea* (*mea*), in which self-fertilization of the heterozygote produces 50% aborted seeds that collapse, accumulate anthocyanin, and do not germinate. This ratio of defective to normal seeds is consistent with a gametophytic control of the defect, because half the haploid gametophytes receive the mutant allele. Heterozygous embryos abort if the mutant allele is derived from the female (Fig. 1A), but develop normally if it is derived from the male (Fig. 1B and Table 1). Embryos derived from mutant eggs abort irrespective of the paternal contribution (*1*). Thus, the *mea* mutant displays maternal-effect embryo lethality (*2*). In flowering plants, embryo development is affected by both the female gametophyte (*3*) and the sporophytic tissue of the parent plant (*4*). The survival of the resultant embryo depends on the presence of a wild-type *MEA* allele in the genome of the female gametophyte.

Fertilization of the egg and central cell generates the diploid zygote and the triploid primary endosperm. Endosperm resulting


Cold Spring Harbor Laboratory, 1 Bungtown Road, Post Office Box 100, Cold Spring Harbor, NY 11724, USA.

*To whom correspondence should be addressed. E-mail: grossnik@cshl.org

†Present address: Graduate Program in Natural Resources, Ohio State University, Columbus, OH 43210–1085, USA.